



Supplement of

Measurement report: Characteristics of nitrogen-containing organics in PM_{2.5} in Ürümqi, northwestern China – differential impacts of combustion of fresh and aged biomass materials

Yi-Jia Ma et al.

Correspondence to: Yu Xu (xuyu360@sjtu.edu.cn)

The copyright of individual parts of the supplement might differ from the article licence.

Table of Contents

Sect. S1–S2

Tables S1–S8

Figures S1–S10

Sect. S1. UPLC-ESI-QToFMS analysis, quality control, and data processing

The organic matter extracted from the filter samples was analyzed using a Waters UPLC-ESI-QToFMS system. Gradient elution with ultrapure water containing 0.1% formic acid (A) and methanol solution containing 0.1% formic acid (B) in a volume ratio was applied in the chromatographic separation of organic compounds. The specific elution linear gradient was as follows: the mobile phase B was initially set at 1% for 1.5 min; increased to 54% and 95% within 6.5 min and 3 min, respectively; then increased to 100% within 1 min and held for 3 min; and finally decreased back to 1% within 0.5 min and held for 2.5 min. The flow rate of the mobile phase was 0.35 mL min⁻¹. One μ L of sample solution was injected into the UPLC system. The optimal instrument operations for sample determination were selected based on the following details, including a capillary voltage of 2.0 kV, a source compensation voltage of 80 V, a sampling cone voltage of 40 V, a source temperature of 115 °C, a desolvanted gas temperature of 450 °C, a cone gas flow rate of 50 L h⁻¹, and a desolvanted gas flow rate of 900 L h⁻¹. The mass calibration was performed by sodium formate solution in both ESI+ and ESI- modes. The mass accuracy was maintained within the whole acquisition period by using a locking spray with the 0.2 ng μ L⁻¹ leucine-enkephalin in a mixed solution (50:50 acetonitrile/water + 0.1% formic acid) as the reference compound (Liu et al., 2020; Lacina et al., 2010).

The recoveries of several standards, including tropinone, sodium camphor sulfonate, potassium phenyl sulfate, sodium methyl sulfate, sodium octyl sulfate, glycolic acid sulfate, lactic acid sulfate, limonaketone sulfate, and α -pinene sulfate,

were detected to evaluate the reliability of the extraction method initially. The recoveries of these standards varied from 84% to 94% (Yang et al., 2023). Thus, we assumed that organic matter in the samples could be effectively extracted in large quantities. Notably, one ppm tropinone and sodium camphor sulfonate were added to the extracts as internal standards of ESI+ and ESI- analysis modes, respectively. The relative standard deviations for the signal intensities of the internal standards were all within 10%, which suggests the stability of the analysis system (Zhao et al., 2022). In addition, mass spectrometry signals in the blank samples were subtracted from those measured in the ambient aerosol samples (Ditto et al., 2020). However, any ion signal occurring in both a sample and its corresponding blank was removed if its signal in the sample was 5 times lower than that in the blank (Ditto et al., 2022).

MassLynx v 4.2 software was used for data acquisition and data processing. All potential molecular formulas for each molecular ion were calculated with a mass tolerance of 5 ppm. Each output molecular formula was allowed to contain certain elements and was limited by the following rules. Specifically, 1–50 of ¹²C, 1–100 of ¹H, 0–50 of ¹⁶O, 0–3 of ¹⁴N, 0–1 of ³²S, and 0–1 of ²³Na were allowed in the molecular formula calculations. The molecular formulas with double bond equivalents (DBE) less than 0 or those that disobeyed the nitrogen rule for even electron ions were excluded from the calculation results (Koch et al., 2007; Wang et al., 2017). The CH compounds were excluded because of their small number (0.43% of the total number of compounds in ESI+) and low signal intensity ($0.33 \pm 0.28\%$ of the total signal intensity in ESI+) being identified in this study. For the compounds with high mass peaks (> 700 Da),

their signal intensities accounted for 1.12% and 1.37% of total signal intensities in ESI+ and ESI-, respectively. Thus, these compounds were also excluded in discussion, as indicated by many previous studies (Wang et al., 2021; Yuan et al., 2023; Xie et al., 2020).

Sect. S2. Parameter calculation

The DBE value can provide information on the number of rings and double bonds in a molecule (Lechtenfeld et al., 2014; Qiao et al., 2020). The DBE value of each identified molecular formula was calculated as follows.

$$\text{DBE} = (2N_C + 2 - N_H + N_N)/2 \quad (1)$$

where the N_C , N_H , and N_N represent the number of C, H, and N atoms in a molecule, respectively.

The carbon oxidation state (OS_C) was first proposed by Kroll et al. (2011) to evaluate the composition evolution of organic compounds that underwent oxidation processes, which was calculated as follows.

$$\text{OS}_C \approx 2 \times N_O/N_C - N_H/N_C \quad (2)$$

where the N_C , N_H , and N_O represent the number of C, H, and O atoms in a molecule, respectively.

The identified compounds can be classified into four subgroups according to their C number and OS_C value, which included semi-volatile oxidized organic aerosol (SV-OOA), low-volatility oxidized organic aerosol (LV-OOA), biomass-burning organic

aerosol (BBOA), and hydrocarbon-like organic aerosol (HOA) (Kroll et al., 2011; Xu et al., 2023; Tong et al., 2016).

The modified aromaticity index (AI_{mod}) can be used to improve the identification and characterization of aromatic-like compounds in aerosol organic matter (Xu et al., 2023; Zhong et al., 2023). The AI_{mod} value was calculated as shown below.

$$\text{AI}_{\text{mod}} = (1 + N_C - 0.5 \times N_O - N_S - 0.5 \times N_N - 0.5 \times N_H) / (N_C - 0.5 \times N_O - N_S - N_N) \quad (3)$$

where the N_C , N_H , N_O , N_N , and N_S correspond to the number of C, H, O, N, and S atoms in a molecular formula, respectively.

Table S1. The mean values (\pm SD) of the major parameters observed in different periods.

Parameter	Annual	Cool period	Warm period
T (°C)	8.56 \pm 13.83	-1.96 \pm 11.26	18.81 \pm 6.40
RH (%)	53.54 \pm 20.30	63.68 \pm 20.20	43.68 \pm 14.78
Wind speed (m s ⁻¹)	2.20 \pm 1.09	2.26 \pm 1.48	2.13 \pm 0.47
pH*	6.34 \pm 1.74	5.80 \pm 1.58	6.86 \pm 1.71
Aerosol liquid water (ALW) (μg m ⁻³)	34.98 \pm 59.61	69.02 \pm 70.11	1.86 \pm 1.90
•OH ($\times 10^5$ molecule cm ⁻³)	13.46 \pm 8.41	9.35 \pm 6.78	17.46 \pm 7.89
PM _{2.5} (μg m ⁻³)	61.38 \pm 56.34	99.44 \pm 58.98	24.35 \pm 9.83
SO ₂ (μg m ⁻³)	9.53 \pm 3.23	10.56 \pm 3.38	8.54 \pm 2.73
NO ₂ (μg m ⁻³)	43.03 \pm 3.23	10.56 \pm 3.38	8.54 \pm 2.73
CO (mg m ⁻³)	1.18 \pm 0.63	1.62 \pm 0.62	0.76 \pm 0.19
O ₃ (μg m ⁻³)	55.34 \pm 29.00	38.83 \pm 23.72	71.41 \pm 25.91
Cl ⁻ (μg m ⁻³)	1.88 \pm 2.30	3.19 \pm 2.64	0.60 \pm 0.57
NO ₃ ⁻ (μg m ⁻³)	10.23 \pm 11.43	17.58 \pm 12.35	3.08 \pm 2.37
SO ₄ ²⁻ (μg m ⁻³)	16.15 \pm 18.76	28.11 \pm 20.53	4.52 \pm 3.06
K ⁺ (μg m ⁻³)	0.36 \pm 0.31	0.51 \pm 0.35	0.21 \pm 0.15
Na ⁺ (μg m ⁻³)	1.38 \pm 2.03	2.15 \pm 2.60	0.62 \pm 0.62
Ca ²⁺ (μg m ⁻³)	3.75 \pm 3.70	4.34 \pm 4.87	3.18 \pm 1.81
Mg ²⁺ (μg m ⁻³)	0.18 \pm 0.19	0.24 \pm 0.25	0.13 \pm 0.08
NH ₄ ⁺ (μg m ⁻³)	7.48 \pm 10.55	13.82 \pm 12.06	1.30 \pm 0.69

Note: *A bias correction of 1 unit was applied for the prediction of aerosol pH (Guo et al., 2015; Wang et al., 2021).

Table S2. The number of compounds in different subgroups, as well as the number fractions and signal intensity fractions of each subgroup.

Mode	Class	Number	Number fraction (%)	Signal intensity fraction (%)
ESI+	CHO	691	36.65	28.76 ± 4.75
	CHON₁₋₃	859	45.57	62.70 ± 6.83
	CHON ₁	329	17.45	35.46 ± 8.92
	CHON ₂	439	23.29	21.94 ± 3.35
	CHON ₃	91	4.83	5.30 ± 1.92
	CHN	335	17.77	9.86 ± 5.22
	CHN ₁	173	9.18	6.64 ± 3.58
	CHN ₂	162	8.59	3.15 ± 2.44
Total	-	1885	100.00	100.00
ESI-	CHO	295	31.12	27.22 ± 8.04
	CHON₁₋₂	143	15.08	28.99 ± 11.52
	CHON ₁	106	11.18	17.41 ± 7.20
	CHON ₂	37	3.90	11.58 ± 7.75
	CHOS	398	41.98	40.36 ± 4.79
	CHON_{1-2S}	112	11.81	3.43 ± 1.84
Total	-	1091	100.00	100.00

Table S3. The arithmetic and peak-intensity-weighted averages of the elemental ratios, DBE values, and X_C values for different compound subgroups in different periods.

Mode Period	Parameters	ESI+				ESI-		
		CHO	CHON	CHN	All	CHO	CHON	All
Cold	O/C ± SD	0.29 ± 0.23	0.30 ± 0.23	-	0.27 ± 0.24	0.58 ± 0.28	0.60 ± 0.26	0.58 ± 0.27
	O/C _w	0.25	0.24	-	0.21	0.48	0.57	0.54
	H/C ± SD	1.63 ± 0.36	1.79 ± 0.31	1.50 ± 0.47	1.69 ± 0.37	1.30 ± 0.36	0.86 ± 0.28	1.18 ± 0.39
	H/C _w	1.65	1.83	1.29	1.71	1.12	0.87	0.97
	N/C ± SD	-	0.12 ± 0.07	0.14 ± 0.07	0.07 ± 0.08	-	0.17 ± 0.08	0.05 ± 0.08
	N/C _w	-	0.10	0.12	0.07	-	0.19	0.11
	DBE ± SD	4.20 ± 2.70	3.81 ± 2.46	5.00 ± 2.93	4.10 ± 2.62	4.68 ± 2.18	6.67 ± 2.05	5.20 ± 2.31
	DBE _w	3.78	2.48	5.65	3.87	5.42	5.61	5.53
	X _C ± SD	2.22 ± 0.68	2.16 ± 0.65	2.28 ± 0.77	2.20 ± 0.68	0.25 ± 0.34	2.67 ± 0.13	2.51 ± 0.31
Warm	X _{Cw}	2.18	2.16	2.52	2.21	2.57	2.63	2.61
	O/C ± SD	0.30 ± 0.22	0.30 ± 0.23	-	0.27 ± 0.23	0.58 ± 0.28	0.59 ± 0.25	0.58 ± 0.27
	O/C _w	0.25	0.22	-	0.21	0.50	0.61	0.56
	H/C ± SD	1.62 ± 0.36	1.79 ± 0.31	1.50 ± 0.47	1.70 ± 0.37	1.29 ± 0.36	0.86 ± 0.29	1.18 ± 0.39
	H/C _w	1.67	1.81	1.43	1.74	1.33	0.82	1.07
	N/C ± SD	-	0.12 ± 0.07	0.14 ± 0.07	0.07 ± 0.08	-	0.17 ± 0.08	0.04 ± 0.08
	N/C _w	-	0.09	0.10	0.07	-	0.23	0.11
	DBE ± SD	4.19 ± 2.70	3.81 ± 2.46	5.00 ± 2.93	4.10 ± 2.63	4.69 ± 2.19	6.64 ± 2.06	5.20 ± 2.31
	DBE _w	3.58	3.86	5.34	3.87	4.73	5.92	5.32
All year	X _C ± SD	2.22 ± 0.69	2.15 ± 0.64	2.29 ± 0.79	2.20 ± 0.68	2.45 ± 0.34	2.67 ± 0.13	2.51 ± 0.32
	X _{Cw}	2.17	2.23	2.42	2.22	2.46	2.65	2.55
	O/C ± SD	0.30 ± 0.23	0.30 ± 0.23	-	0.27 ± 0.24	0.58 ± 0.28	0.60 ± 0.25	0.58 ± 0.27
	O/C _w	0.25	0.23	-	0.21	0.49	0.58	0.54
	H/C ± SD	1.63 ± 0.36	1.79 ± 0.31	1.50 ± 0.47	1.70 ± 0.37	1.29 ± 0.36	0.86 ± 0.28	1.18 ± 0.39
	H/C _w	1.66	1.82	1.34	1.73	1.19	0.85	1.00
	N/C ± SD	-	0.12 ± 0.07	0.14 ± 0.07	0.07 ± 0.08	-	0.17 ± 0.08	0.04 ± 0.08
	N/C _w	-	0.10	0.11	0.07	-	0.20	0.11
	DBE ± SD	4.19 ± 2.70	3.81 ± 2.46	5.00 ± 2.93	4.09 ± 2.63	4.68 ± 2.18	6.67 ± 2.05	5.20 ± 2.31
	DBE _w	3.66	3.71	5.54	3.87	5.18	5.70	5.47
	X _C ± SD	2.21 ± 0.69	2.16 ± 0.64	2.29 ± 0.77	2.20 ± 0.68	2.45 ± 0.34	2.67 ± 0.13	2.51 ± 0.31
	X _{Cw}	2.17	2.20	2.48	2.22	2.53	0.64	2.59

Table S4. Characteristics of the observed CHON compounds with relatively high signal intensity compared to other CHON compounds in ESI+ mode in the warm period.

Formula	N	O/C	H/C	N/C	O/N	DBE	Percentage (%)	Precursor
C ₁₆ H ₃₃ ON ^a	1	0.063	2.063	0.063	1	1	10.25 ± 1.03	Palmitic acid
C ₁₆ H ₃₁ ON ^a	1	0.063	1.938	0.063	1	2	0.25 ± 0.09	Palmitoleic acid
C ₁₆ H ₂₉ O ₆ N ^b	1	0.375	1.813	0.063	6	3	0.0012 ± 0.0014	Palmitoleic acid
C ₁₆ H ₂₈ O ₄ N ₂ ^d	2	0.250	1.750	0.125	2	4	0.025 ± 0.011	Palmitoleic acid
C ₁₆ H ₃₀ O ₄ N ₂ ^d	2	0.250	1.875	0.125	2	3	0.0031 ± 0.0011	Palmitoleic acid
C ₁₆ H ₃₂ O ₅ N ₂ ^c	2	0.313	2.000	0.125	2.5	2	0.043 ± 0.021	Palmitoleic acid
C ₁₈ H ₃₇ ON ^a	1	0.056	2.056	0.056	1	1	16.79 ± 2.81	Stearic acid
C ₁₈ H ₃₅ ON ^a	1	0.056	1.944	0.056	1	2	6.85 ± 1.38	Oleic acid
C ₁₈ H ₃₃ ON ^a	1	0.056	1.833	0.056	1	3	0.77 ± 0.28	Linoleic acid
C ₁₈ H ₃₁ ON ^a	1	0.056	1.722	0.056	1	4	7.59 ± 0.94	α-Linolenic acid
C ₁₈ H ₃₅ O ₆ N ^b	1	0.333	1.944	0.056	6	2	0.039 ± 0.025	Oleic acid
C ₁₈ H ₃₀ O ₄ N ₂ ^d	2	0.222	1.667	0.111	2	5	0.082 ± 0.031	Linoleic acid or α-Linolenic acid
C ₁₈ H ₃₂ O ₄ N ₂ ^d	2	0.222	1.778	0.111	2	4	0.16 ± 0.09	Oleic acid or Linoleic acid
C ₁₈ H ₃₄ O ₄ N ₂ ^d	2	0.222	1.889	0.111	2	3	0.063 ± 0.022	Oleic acid
C ₁₈ H ₃₄ O ₅ N ₂ ^c	2	0.278	1.889	0.111	2.5	3	0.019 ± 0.0092	Oleic acid
C ₁₈ H ₃₆ O ₅ N ₂ ^c	2	0.278	2.000	0.111	2.5	2	0.043 ± 0.012	Oleic acid
C ₂₀ H ₃₃ ON ^a	1	0.050	1.650	0.050	1	5	12.79 ± 2.01	Arachidonic acid
C ₂₀ H ₄₁ ON ^a	1	0.050	2.050	0.050	1	1	1.23 ± 0.72	Arachidic acid
C ₂₀ H ₃₂ O ₄ N ₂ ^d	2	0.200	1.600	0.100	2	6	0.062 ± 0.028	Arachidonic acid
Total	-	-	-	-	-	-	57.06 ± 7.75	-

^aAmides; ^bOrganic nitrates; ^cNitrooxy amides; and ^dNitrooxy nitriles. These compounds were identified or inferred based on their MS/MS fragments or the molecular formulae of the products obtained from Figure 5.

Table S5. Mass spectrometry characteristics of the identified amides and nitriles in samples.

Observed mass (Da)	Theoretical mass (Da)	Molecular formula (M+H)	Molecular formula (M)	RT (min.)	Mass error (ppm)	Major MS/MS fragments
Amides						
254.2489	254.2484	C ₁₆ H ₃₂ ON	C ₁₆ H ₃₁ ON	11.34	2.0	237.1984, 184.1111, 237.0741, 223.0591, 208.0374, 165.0713, 153.0675, 141.0694, 128.0609
256.2639	256.2640	C ₁₆ H ₃₄ ON	C ₁₆ H ₃₃ ON	11.36	-0.4	239.2147, 88.0769, 102.0916, 116.1066, 74.0605, 130.1226, 144.1378, 69.0689,
278.2481	278.2484	C ₁₈ H ₃₂ ON	C ₁₈ H ₃₁ ON	12.31	-1.1	261.1989, 222.1221, 201.0505, 191.1586, 150.1176, 132.0851
280.2642	280.2640	C ₁₈ H ₃₄ ON	C ₁₈ H ₃₃ ON	12.21	0.7	263.2146, 248.0794, 235.2289, 212.0505, 165.1446, 152.1295, 109.0756, 91.0585
282.2791	282.2797	C ₁₈ H ₃₆ ON	C ₁₈ H ₃₅ ON	12.40	-2.1	265.2512, 134.0965, 83.0848, 97.1021, 69.0706, 121.1015, 107.0854, 240.2695
284.2955	284.2953	C ₁₈ H ₃₈ ON	C ₁₈ H ₃₇ ON	12.68	0.7	267.2434, 88.0769, 102.0916, 116.1066, 130.1226, 74.0594, 83.0848, 144.1378,
304.2633	304.2640	C ₂₀ H ₃₄ ON	C ₂₀ H ₃₃ ON	12.49	-2.3	287.2122, 272.1965, 259.1723, 247.1455, 213.0959, 189.1388, 161.1080, 134.0965
Nitriles						
238.2536	238.2535	C ₁₆ H ₃₂ N	C ₁₆ H ₃₁ N	11.37	0.4	223.1234, 209.1188, 195.1020, 180.0611, 165.0710, 152.0614, 128.0627, 119.0899, 115.0569, 100.1183, 91.0579, 77.0556
260.2375	260.2378	C ₁₈ H ₃₀ N	C ₁₈ H ₂₉ N	11.55	-1.2	230.1917, 216.1740, 204.1752, 191.1672, 175.1375, 146.0971, 132.0809, 120.0816, 106.0653, 91.0527
262.2537	262.2535	C ₁₈ H ₃₂ N	C ₁₈ H ₃₁ N	11.73	0.8	106.0653, 120.0793, 177.1522, 190.1587, 204.1752
264.2686	264.2691	C ₁₈ H ₃₄ N	C ₁₈ H ₃₃ N	12.44	-1.9	253.0890, 207.1060, 163.1476, 149.1320, 135.1171, 121.1015, 109.0997, 107.0854, 95.0846, 81.0683, 79.0529, 67.0537
266.2841	266.2848	C ₁₈ H ₃₆ N	C ₁₈ H ₃₅ N	12.76	-2.6	253.0926, 208.1171, 195.0991, 157.0899, 145.1043, 128.0673, 115.0569, 95.0860, 67.0547
290.2848	290.2848	C ₂₀ H ₃₆ N	C ₂₀ H ₃₅ N	12.62	0.0	218.1910, 204.1572, 191.1672, 134.0965, 120.0816, 106.0653

Table S6. Characteristics of the observed CHON compounds with relatively high signal intensity compared to other CHON compounds in ESI– mode in the cold period.

Formula	N	DBE	Percentage (%)	Classification	Potential origin	Reference
C ₆ H ₅ O ₃ N	1	5	17.39	Nitrophenol	Biomass burning	(Salvador et al., 2021; Cai et al., 2023; Xie et al., 2019)
C ₆ H ₄ O ₅ N ₂	2	6	13.69	Dinitrophenol	Biomass burning	(Salvador et al., 2021; Cai et al., 2023)
C ₇ H ₇ O ₃ N	1	5	13.13	Nitrophenol	Biomass burning	(Salvador et al., 2021; Cai et al., 2023)
C ₆ H ₅ O ₄ N	1	5	7.16	Nitrocatechol	Wood-burning SOA	(Salvador et al., 2023; Xie et al., 2019; Iinuma et al., 2010)
C ₇ H ₆ O ₅ N ₂	2	6	6.42	Dinitrophenol	Biomass burning	(Salvador et al., 2021)
C ₈ H ₉ O ₃ N	1	5	5.40	Nitrophenol	Biomass burning	(Salvador et al., 2021)
C ₇ H ₇ O ₄ N	1	5	5.20	Nitrocatechol	Wood-burning SOA	(Salvador et al., 2023; Xie et al., 2019; Iinuma et al., 2010)
C ₁₀ H ₇ O ₃ N	1	8	3.17	Nitrophenol	Biomass burning	(Salvador et al., 2021; Xie et al., 2019)
C ₇ H ₅ O ₅ N	1	6	2.69	Nitrosalicylic acid	Biomass burning	(Cai et al., 2023)
C ₇ H ₆ O ₆ N ₂	2	6	2.67	Dinitrophenol	Biomass burning, aged BBOAs	(Salvador et al., 2021; Bao et al., 2023)
C ₇ H ₄ O ₇ N ₂	2	7	2.29	-	Photosensitized oxidation	(Mabato et al., 2022)
C ₈ H ₉ O ₄ N	1	5	1.91	-	Biomass burning	(Xie et al., 2019)
Total	-	-	81.12	-	-	-

Table S7. Characteristics of the observed CHN compounds with relatively high signal intensity compared to other CHN compounds in ESI+ mode in the cold period.

Formula	N	N/C	DBE	Percentage (%)	Proposed compound name	Potential origin	Reference
C ₁₀ H ₁₄ N ₂	2	0.20	5	9.48	Nicotine	Cigarette	(Qi et al., 2020; Qi et al., 2019)
C ₁₀ H ₉ N ^b	1	0.10	7	7.71	Alkyl quinolene	Biomass burning	(Laskin et al., 2009)
C ₁₁ H ₁₁ N ^b	1	0.091	7	6.99	2,8-Dimethylquinoline	-	(Yao et al., 2016)
C ₉ H ₁₃ N ^a	1	0.11	4	6.09	Dimethylbenzylamine or N-Ethyl-N-methylaniline	-	(Ditto et al., 2022; Witte et al., 1986)
C ₇ H ₉ N ^a	1	0.14	4	5.96	2,4-Lutidine	-	(Zhang et al., 2016)
C ₉ H ₇ N ^b	1	0.11	7	5.82	Quinoline	Fossil fuel combustion, vehicular exhaust	(Yao et al., 2016; Lyu et al., 2019; Rogge et al., 1993)
C ₁₃ H ₉ N ^c	1	0.077	10	3.71	Acridine	Dung and brushwood burning, straw residue burning	(Wang et al., 2017; Fleming et al., 2018)
C ₁₃ H ₁₁ N	1	0.070	9	3.54	C1-Azafluorene	straw residue burning	(Vila et al., 2020; Wang et al., 2017)
C ₁₂ H ₁₃ N ^b	1	0.083	7	3.47	-	dung cookfire emissions	(Fleming et al., 2018)
C ₁₅ H ₁₃ N ^c	1	0.067	10	3.12	Aromatic Bases	Petroleum, Coal	(Herod et al., 2005)
C ₁₀ H ₁₅ N ^a	1	0.10	4	2.96	Benzenamine	-	(Atkinson et al., 1987)
C ₁₁ H ₂₀ N ₂	2	0.18	3	2.65	-	Dung and brushwood burning	(Fleming et al., 2018)
C ₁₄ H ₁₁ N ^c	1	0.071	10	2.62	9-Amioanthracene	-	-
C ₉ H ₁₀ N ₂	2	0.22	6	1.76	-	Straw residue burning, dung and brushwood burning	(Wang et al., 2017; Fleming et al., 2018)
C ₈ H ₁₉ N	1	0.13	0	1.50	Dibutylamine	-	(Ditto et al., 2022; Pankow and Asher, 2008)
C ₁₃ H ₁₅ N ^b	1	0.077	7	1.30	-	Petroleum	(Axe and Bailey, 1938)
C ₈ H ₁₁ N ^a	1	0.13	4	1.20	Phenethylamine	-	(Yao et al., 2016)
C ₈ H ₈ N ₂	2	0.25	6	1.14	-	Straw residue burning, biomass burning	(Laskin et al., 2009; Wang et al., 2017)
Total	-	-	-	70.99	-	-	-

^a C₅H₅N(CH₂)_n ^b C₉H₇N(CH₂)_n ^c C₁₃H₉N(CH₂)_n

Table S8. Compound categorization according to elemental ratio and AI_{mod} value

Classification	Classification	H/C	O/C	AI _{mod}	Reference
Saturated-like molecules	Sa	≥ 2.0	-	< 0.5	
Unsaturated aliphatic-like molecules	UA _O -poor	1.5–2.0	≤ 0.5	< 0.5	(Koch and Dittmar, 2006; Merder et al., 2020)
	UA _O -rich	1.5–2.0	> 0.5	< 0.5	
Highly unsaturated-like molecules	HU _O -poor	< 1.5	≤ 0.5	< 0.5	(Koch and Dittmar, 2006; Merder et al., 2020)
	HU _O -rich	< 1.5	> 0.5	< 0.5	
Highly aromatic-like molecules	HA _O -poor	-	≤ 0.5	0.5–0.66	(Koch and Dittmar, 2006; Merder et al., 2020)
	HA _O -rich	-	> 0.5	0.5–0.66	
Polycyclic aromatic-like molecules	PA _O -poor	-	≤ 0.5	> 0.66	(Koch and Dittmar, 2006; Merder et al., 2020)
	PA _O -rich	-	> 0.5	> 0.66	

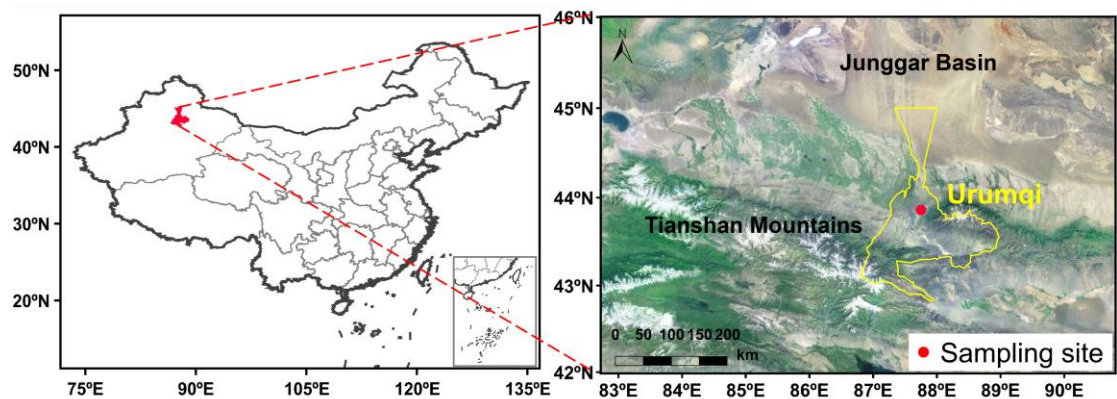


Figure S1. The location showing the PM_{2.5} sampling site in Urumqi. The map was derived from ©MeteoInfoMap (version 3.6.2) (Chinese Academy of Meteorological Sciences, China).

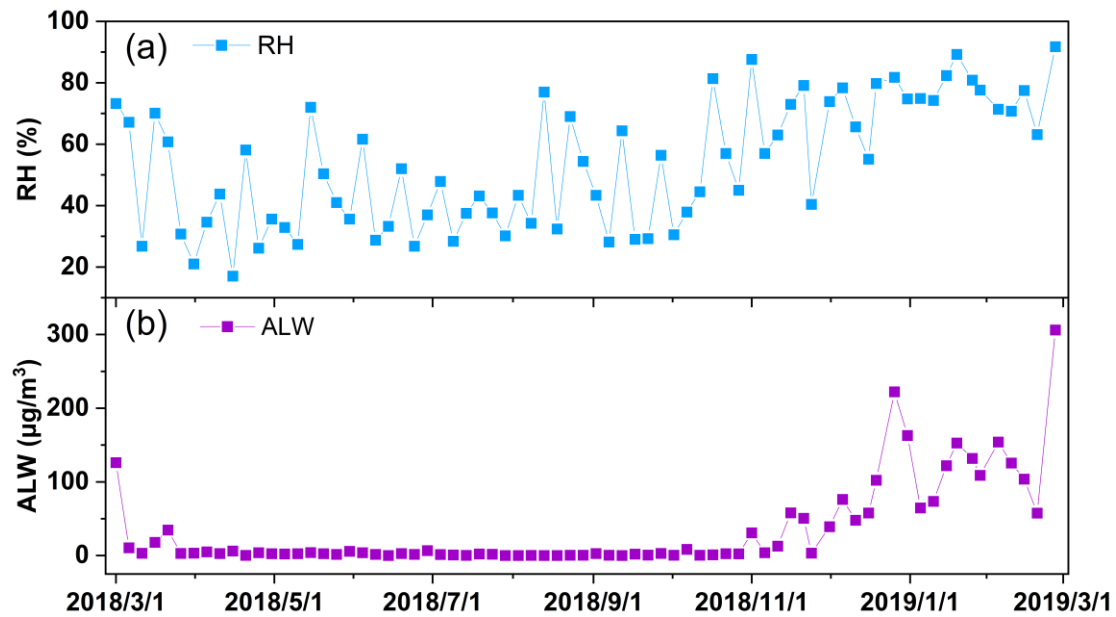


Figure S2. Temporal variations in (a) RH value and (b) ALW concentration.

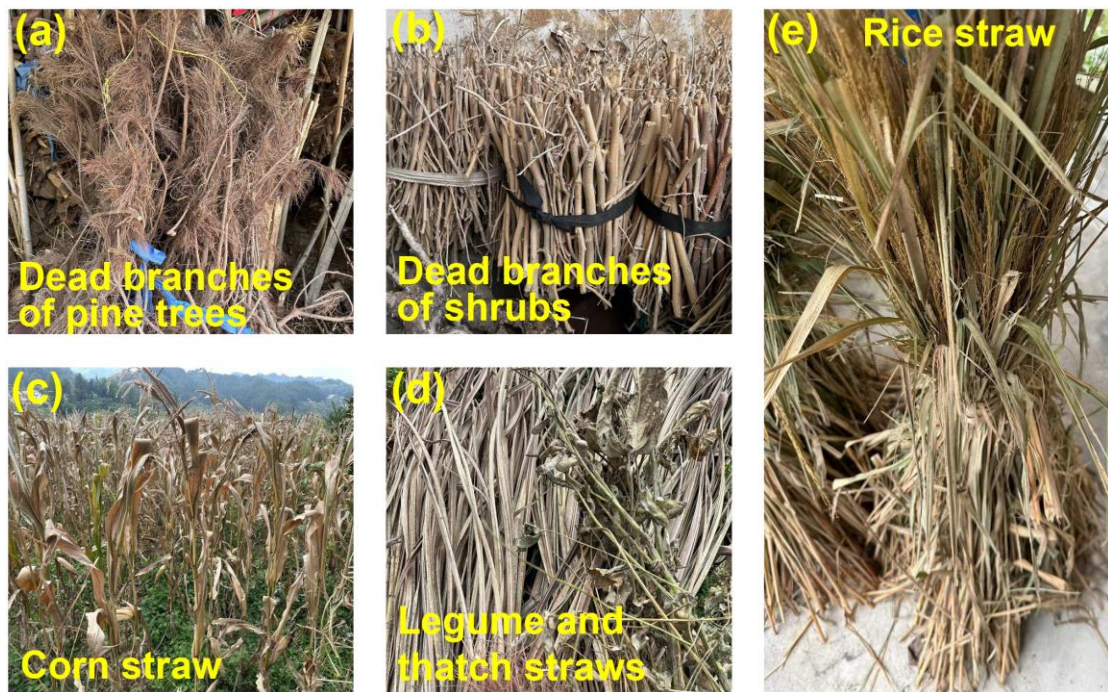


Figure S3. Exhibition of several old-age biomass materials. (a) Dead branches of pine trees, (b) dead branches of shrubs, (c) corn straw, (d) legume and thatch straws, and (e) rice straw. All photos were taken by the corresponding author.

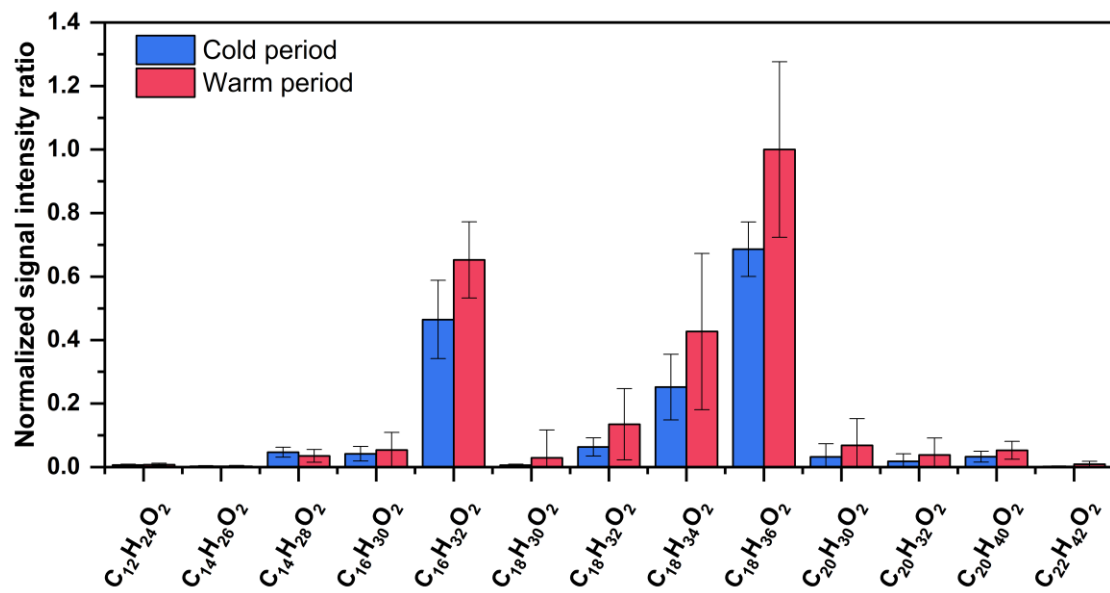


Figure S4. The normalized signal intensity ratio distributions of fatty acid analogs detected in PM_{2.5} collected from the cold and warm periods. The normalization was conducted based on the one with the highest signal intensity.

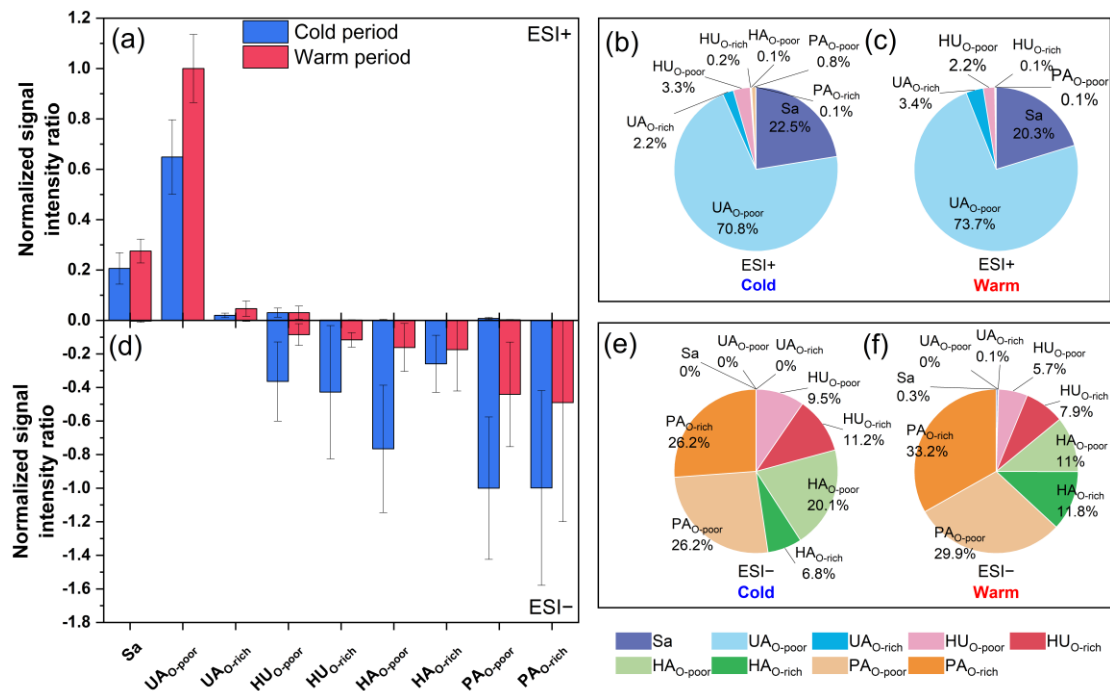


Figure S5. The normalized signal intensity ratio distributions of saturated-like (Sa), unsaturated aliphatic-like (UA), highly unsaturated-like (HU), highly aromatic-like (HA), and polycyclic aromatic-like (PA) compounds detected in (a) ESI+ and (d) ESI- modes in PM_{2.5} collected from the cold and warm periods. The signal intensity fractions of classified compounds in (b and c) ESI+ and (e and f) ESI- in different periods. The normalization was conducted based on the one with the highest signal intensity.

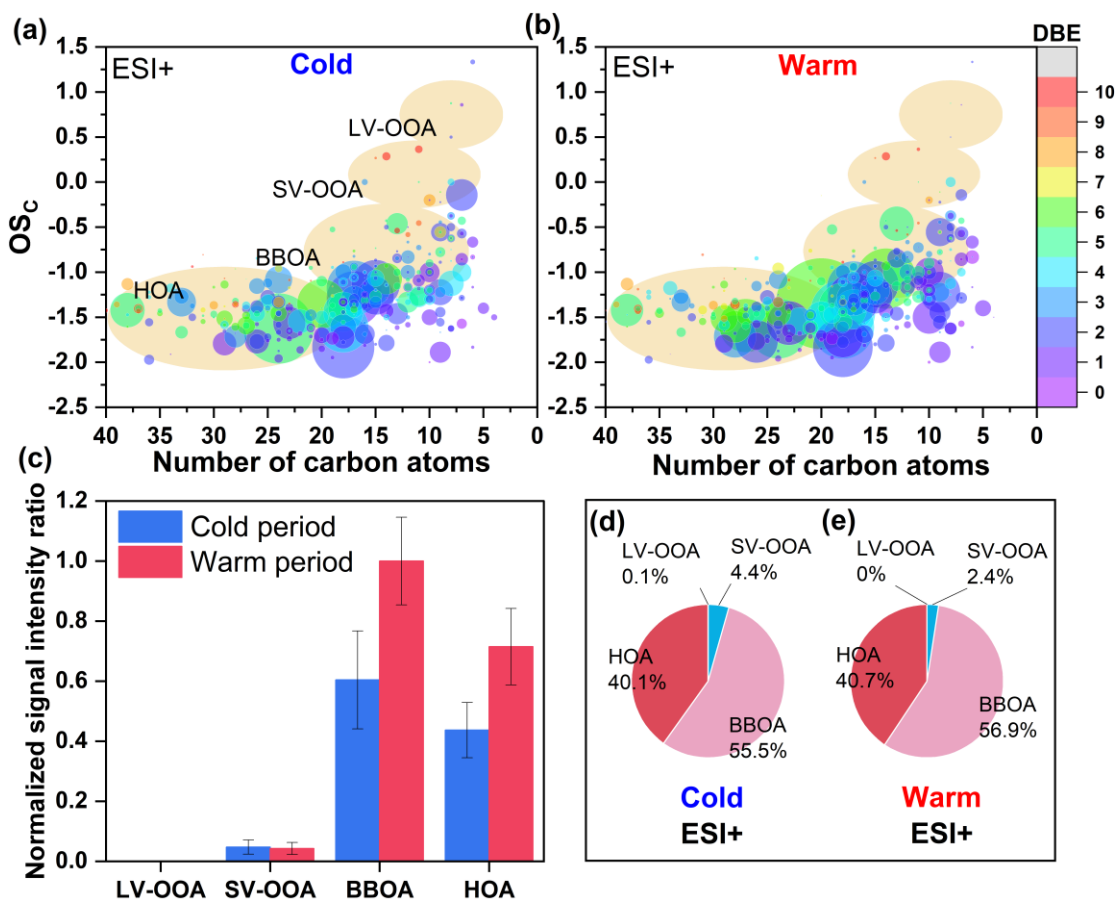


Figure S6. OSc values of CHON molecules detected in ESI+ mode in PM_{2.5} collected in the (a) cold and (b) warm periods. The size and color of the circle indicate the mean signal intensity and DBE value of compounds, respectively. The light-orange background indicates the areas of low-volatility oxidized OA (LV-OOA), semivolatile oxidized OA (SV-OOA), biomass burning-like OA (BBOA), and hydrocarbon-like OA (HOA) (Kroll et al., 2011), according to which (c) the normalized signal intensity of classified compounds was calculated for samples from different periods. The signal intensity fractions of classified compounds in the (d) cold and (e) warm periods. The normalization was conducted based on the one with the highest signal intensity.

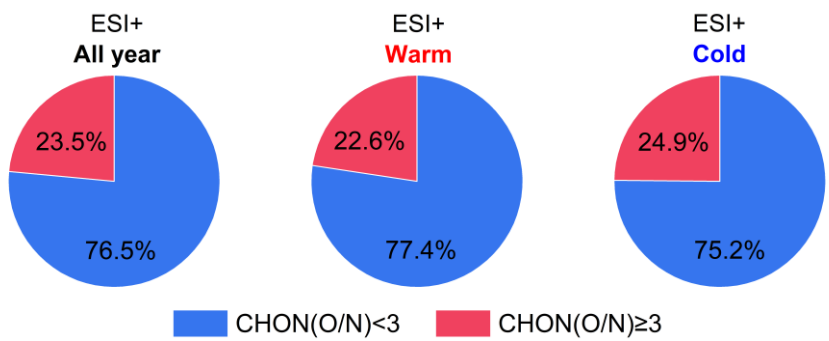


Figure S7. Average signal intensity fraction distributions of CHON compounds with $\text{O/N} < 3$ and $\text{O/N} \geq 3$ in ESI+ in different periods.

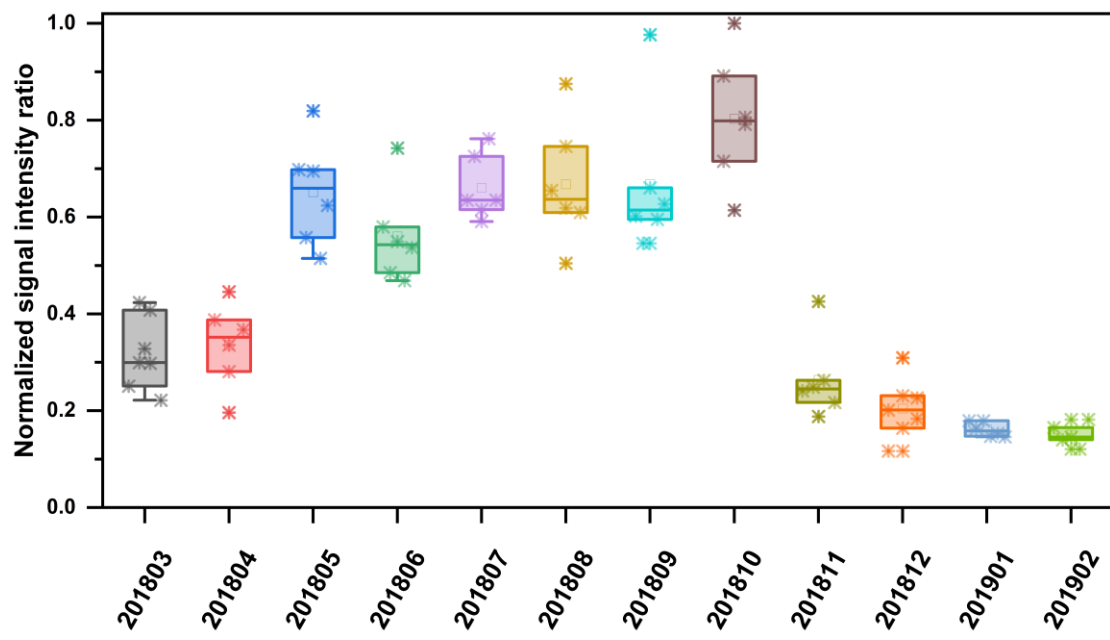


Figure S8. Temporal variations in the normalized signal intensity ratio of the C_{16–20} amide species. The normalization was conducted based on the one with the highest signal intensity.

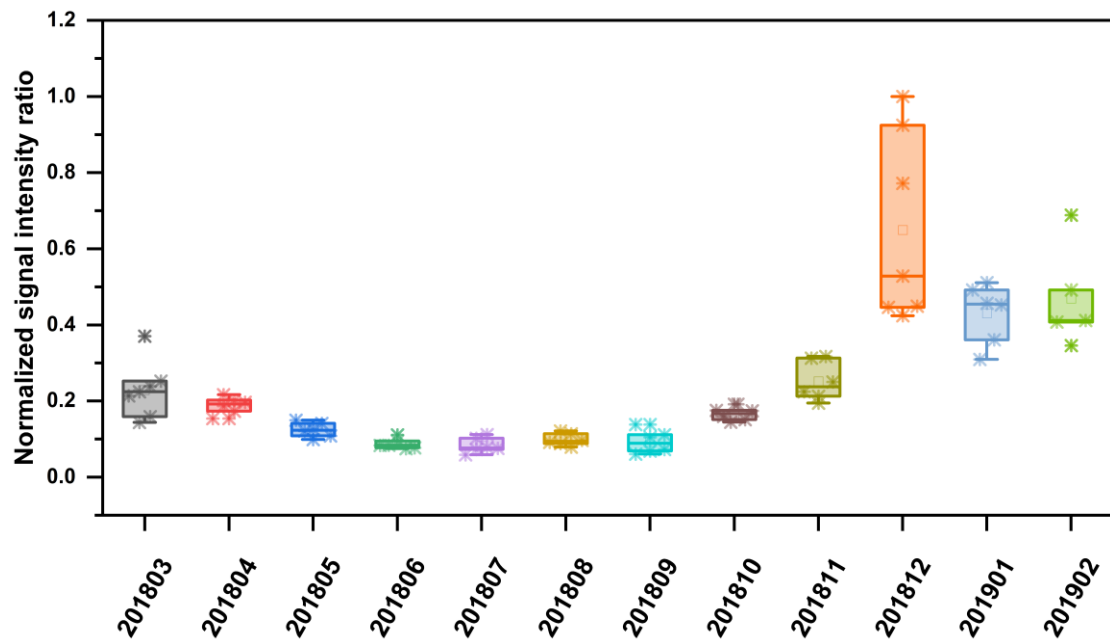


Figure S9. Temporal variations in the normalized signal intensity ratio of aromatic-like CHN species. The normalization was conducted based on the one with the highest signal intensity.

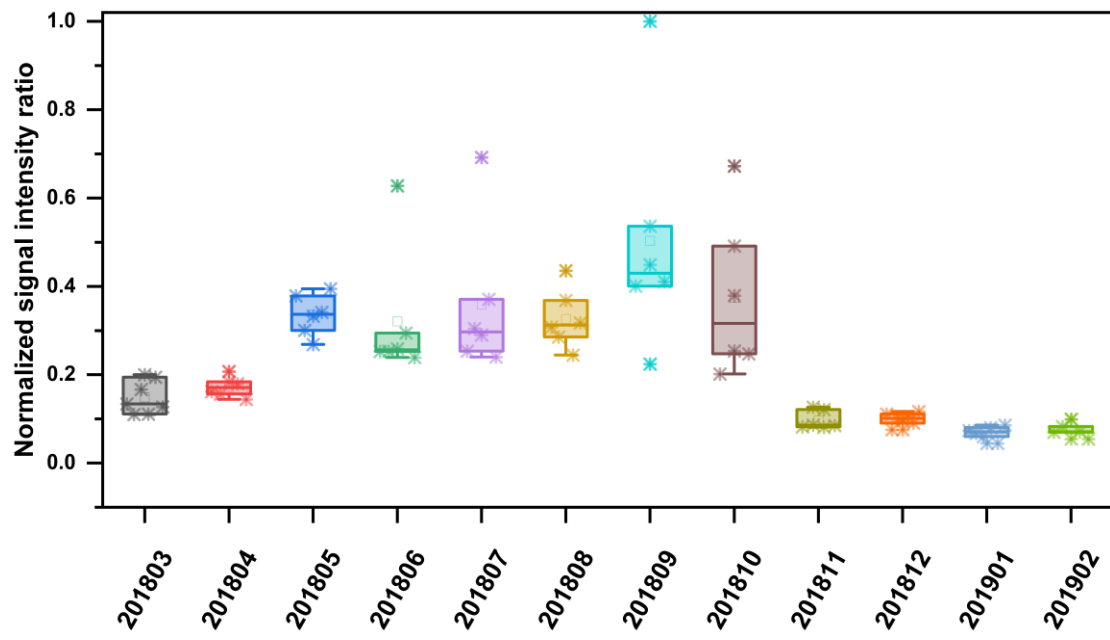


Figure S10. Temporal variations in the normalized signal intensity ratio of alkyl nitriles.

The normalization was conducted based on the one with the highest signal intensity.

REFERENCES

- Atkinson, R., Tuazon, E. C., Wallington, T. J., Aschmann, S. M., Arey, J., Winer, A. M., and Pitts, J. N.: Atmospheric chemistry of aniline, N,N-dimethylaniline, pyridine, 1,3,5-triazine, and nitrobenzene, Environ. Sci. Technol., 21, 64-72, <https://doi.org/10.1021/es00155a007>, 1987.
- Axe, W. N. and Bailey, J. R.: The Nitrogen Compounds in Petroleum Distillates. XIII. Isolation of Four Quinoline Homologs and Two Aromatic Bases of Probable Trinuclear Cyclic Structure¹, J. Am. Chem. Soc., 60, 3028-3032, <https://doi.org/10.1021/ja01279a059>, 1938.
- Bao, M., Zhang, Y. L., Cao, F., Hong, Y., Lin, Y. C., Yu, M., Jiang, H., Cheng, Z., Xu, R., and Yang, X.: Impact of fossil and non-fossil fuel sources on the molecular compositions of water-soluble humic-like substances in PM_{2.5} at a suburban site of Yangtze River Delta, China, Atmos. Chem. Phys., 23, 8305-8324, <https://doi.org/10.5194/acp-23-8305-2023>, 2023.
- Cai, Y., Ye, C., Chen, W., Hu, W., Song, W., Peng, Y., Huang, S., Qi, J., Wang, S., Wang, C., Wu, C., Wang, Z., Wang, B., Huang, X., He, L., Gligorovski, S., Yuan, B., Shao, M., and Wang, X.: The important contribution of secondary formation and biomass burning to oxidized organic nitrogen (OON) in a polluted urban area: insights from in situ measurements of a chemical ionization mass spectrometer (CIMS), Atmos. Chem. Phys., 23, 8855-8877, <https://doi.org/10.5194/acp-23-8855-2023>, 2023.
- Ditto, J. C., Machesky, J., and Gentner, D. R.: Analysis of reduced and oxidized nitrogen-containing organic compounds at a coastal site in summer and winter,

Atmos. Chem. Phys., 22, 3045-3065, <https://doi.org/10.5194/acp-22-3045-2022>,
2022.

Ditto, J. C., Joo, T., Slade, J. H., Shepson, P. B., Ng, N. L., and Gentner, D. R.:
Nontargeted Tandem Mass Spectrometry Analysis Reveals Diversity and
Variability in Aerosol Functional Groups across Multiple Sites, Seasons, and
Times of Day, Environ. Sci. Technol. Lett., 7, 60-69,
<https://doi.org/10.1021/acs.estlett.9b00702>, 2020.

Fleming, L. T., Lin, P., Laskin, A., Laskin, J., Weltman, R., Edwards, R. D., Arora, N.
K., Yadav, A., Meinardi, S., Blake, D. R., Pillarisetti, A., Smith, K. R., and
Nizkorodov, S. A.: Molecular composition of particulate matter emissions from
dung and brushwood burning household cookstoves in Haryana, India, Atmos.
Chem. Phys., 18, 2461-2480, <https://doi.org/10.5194/acp-18-2461-2018>, 2018.

Guo, H., Xu, L., Bougiatioti, A., Cerully, K. M., Capps, S. L., Hite Jr, J. R., Carlton, A.
G., Lee, S. H., Bergin, M. H., Ng, N. L., Nenes, A., and Weber, R. J.: Fine-particle
water and pH in the southeastern United States, Atmos. Chem. Phys., 15, 5211-
5228, <https://doi.org/10.5194/acp-15-5211-2015>, 2015.

Herod, A. A., Millan, M., Morgan, T., Li, W., Feng, J., and Kandiyoti, R.: Positive-Ion
Electrospray Ionisation Mass Spectrometry of Acetone- and Acetonitrile-Soluble
Fractions of Coal-Derived Liquids, Eur. J. Mass Spectrom., 11, 429-442,
<https://doi.org/10.1255/ejms.768>, 2005.

Iinuma, Y., Böge, O., Gräfe, R., and Herrmann, H.: Methyl-Nitrocatechols:
Atmospheric Tracer Compounds for Biomass Burning Secondary Organic

Aerosols, Environ. Sci. Technol., 44, 8453-8459,

<https://doi.org/10.1021/es102938a>, 2010.

Koch, B. P. and Dittmar, T.: From mass to structure: an aromaticity index for high-resolution mass data of natural organic matter, Rapid Commun. Mass Spectrom., 20, 926-932, <https://doi.org/10.1002/rcm.2386>, 2006.

Koch, B. P., Dittmar, T., Witt, M., and Kattner, G.: Fundamentals of Molecular Formula Assignment to Ultrahigh Resolution Mass Data of Natural Organic Matter, Anal. Chem., 79, 1758-1763, <https://doi.org/10.1021/ac061949s>, 2007.

Kroll, J. H., Donahue, N. M., Jimenez, J. L., Kessler, S. H., Canagaratna, M. R., Wilson, K. R., Altieri, K. E., Mazzoleni, L. R., Wozniak, A. S., Bluhm, H., Mysak, E. R., Smith, J. D., Kolb, C. E., and Worsnop, D. R.: Carbon oxidation state as a metric for describing the chemistry of atmospheric organic aerosol, Nat. Chem., 3, 133-139, <https://doi.org/10.1038/nchem.948>, 2011.

Lacina, O., Urbanova, J., Poustka, J., and Hajslova, J.: Identification/quantification of multiple pesticide residues in food plants by ultra-high-performance liquid chromatography-time-of-flight mass spectrometry, J. Chromatogr. A, 1217, 648-659, <https://doi.org/10.1016/j.chroma.2009.11.098>, 2010.

Laskin, A., Smith, J. S., and Laskin, J.: Molecular Characterization of Nitrogen-Containing Organic Compounds in Biomass Burning Aerosols Using High-Resolution Mass Spectrometry, Environ. Sci. Technol., 43, 3764-3771, <https://doi.org/10.1021/es803456n>, 2009.

Lechtenfeld, O. J., Kattner, G., Flerus, R., McCallister, S. L., Schmitt-Kopplin, P., and

Koch, B. P.: Molecular transformation and degradation of refractory dissolved organic matter in the Atlantic and Southern Ocean, *Geochim. Cosmochim. Acta*, 126, 321-337, <https://doi.org/10.1016/j.gca.2013.11.009>, 2014.

Liu, F.-J., Jiang, Y., Li, P., Liu, Y.-D., Yao, Z.-P., Xin, G.-Z., and Li, H.-J.: Untargeted metabolomics coupled with chemometric analysis reveals species-specific steroid alkaloids for the authentication of medicinal *Fritillariae Bulbus* and relevant products, *J. Chromatogr. A*, 1612, 460630, <https://doi.org/10.1016/j.chroma.2019.460630>, 2020.

Lyu, R., Shi, Z., Alam, M. S., Wu, X., Liu, D., Vu, T. V., Stark, C., Fu, P., Feng, Y., and Harrison, R. M.: Insight into the composition of organic compounds ($\geq C_6$) in PM_{2.5} in wintertime in Beijing, China, *Atmos. Chem. Phys.*, 19, 10865-10881, <https://doi.org/10.5194/acp-19-10865-2019>, 2019.

Mabato, B. R. G., Lyu, Y., Ji, Y., Li, Y. J., Huang, D. D., Li, X., Nah, T., Lam, C. H., and Chan, C. K.: Aqueous secondary organic aerosol formation from the direct photosensitized oxidation of vanillin in the absence and presence of ammonium nitrate, *Atmos. Chem. Phys.*, 22, 273-293, <https://doi.org/10.5194/acp-22-273-2022>, 2022.

Merder, J., Freund, J. A., Feudel, U., Hansen, C. T., Hawkes, J. A., Jacob, B., Klaproth, K., Niggemann, J., Noriega-Ortega, B. E., Osterholz, H., Rossel, P. E., Seidel, M., Singer, G., Stubbins, A., Waska, H., and Dittmar, T.: ICBM-OCEAN: Processing Ultrahigh-Resolution Mass Spectrometry Data of Complex Molecular Mixtures, *Anal. Chem.*, 92, 6832-6838, <https://dx.doi.org/10.1021/acs.analchem.9b05659>,

2020.

Pankow, J. F. and Asher, W. E.: SIMPOL.1: a simple group contribution method for predicting vapor pressures and enthalpies of vaporization of multifunctional organic compounds, *Atmos. Chem. Phys.*, 8, 2773-2796, <https://doi.org/10.5194/acp-8-2773-2008>, 2008.

Qi, L., Chen, M., Stefenelli, G., Pospisilova, V., Tong, Y., Bertrand, A., Hueglin, C., Ge, X., Baltensperger, U., Prévôt, A. S. H., and Slowik, J. G.: Organic aerosol source apportionment in Zurich using an extractive electrospray ionization time-of-flight mass spectrometer (EESI-TOF-MS) – Part 2: Biomass burning influences in winter, *Atmos. Chem. Phys.*, 19, 8037-8062, <https://doi.org/10.5194/acp-19-8037-2019>, 2019.

Qi, L., Vogel, A. L., Esmaeilirad, S., Cao, L., Zheng, J., Jaffrezo, J. L., Fermo, P., Kasper-Giebl, A., Daellenbach, K. R., Chen, M., Ge, X., Baltensperger, U., Prévôt, A. S. H., and Slowik, J. G.: A 1-year characterization of organic aerosol composition and sources using an extractive electrospray ionization time-of-flight mass spectrometer (EESI-TOF), *Atmos. Chem. Phys.*, 20, 7875-7893, <https://doi.org/10.5194/acp-20-7875-2020>, 2020.

Qiao, W., Guo, H., He, C., Shi, Q., Xiu, W., and Zhao, B.: Molecular Evidence of Arsenic Mobility Linked to Biodegradable Organic Matter, *Environ. Sci. Technol.*, 54, 7280-7290, <https://dx.doi.org/10.1021/acs.est.0c00737>, 2020.

Rogge, W. F., Hildemann, L. M., Mazurek, M. A., Cass, G. R., and Simoneit, B. R. T.: Sources of fine organic aerosol. 2. Noncatalyst and catalyst-equipped automobiles

and heavy-duty diesel trucks, Environ. Sci. Technol., 27, 636-651,
<https://doi.org/10.1021/es00041a007>, 1993.

Salvador, C. M. G., Tang, R., Priestley, M., Li, L., Tsiligiannis, E., Le Breton, M., Zhu, W., Zeng, L., Wang, H., Yu, Y., Hu, M., Guo, S., and Hallquist, M.: Ambient nitro-aromatic compounds – biomass burning versus secondary formation in rural China, Atmos. Chem. Phys., 21, 1389-1406, <https://doi.org/10.5194/acp-21-1389-2021>, 2021.

Tong, H., Kourtchev, I., Pant, P., Keyte, I. J., O'Connor, I. P., Wenger, J. C., Pope, F. D., Harrison, R. M., and Kalberer, M.: Molecular composition of organic aerosols at urban background and road tunnel sites using ultra-high resolution mass spectrometry, Faraday Discuss., 189, 51-68, <https://doi.org/10.1039/C5FD00206K>, 2016.

Vila, J., Tian, Z., Wang, H., Bodnar, W., and Aitken, M. D.: Isomer-selective biodegradation of high-molecular-weight azaarenes in PAH-contaminated environmental samples, Sci. Total Environ., 707, 135503, <https://doi.org/10.1016/j.scitotenv.2019.135503>, 2020.

Wang, Y., Hu, M., Lin, P., Guo, Q., Wu, Z., Li, M., Zeng, L., Song, Y., Zeng, L., Wu, Y., Guo, S., Huang, X., and He, L.: Molecular Characterization of Nitrogen-Containing Organic Compounds in Humic-like Substances Emitted from Straw Residue Burning, Environ. Sci. Technol., 51, 5951-5961, <https://doi.org/10.1021/acs.est.7b00248>, 2017.

Wang, Y., Hu, M., Hu, W., Zheng, J., Niu, H., Fang, X., Xu, N., Wu, Z., Guo, S., Wu,

- Y., Chen, W., Lu, S., Shao, M., Xie, S., Luo, B., and Zhang, Y.: Secondary Formation of Aerosols Under Typical High-Humidity Conditions in Wintertime Sichuan Basin, China: A Contrast to the North China Plain, *J. Geophys. Res.-Atmos.*, 126, e2021JD034560, <https://doi.org/10.1029/2021JD034560>, 2021.
- Witte, F., Urbanik, E., and Zetzsch, C.: Temperature dependence of the rate constants for the addition of hydroxyl to benzene and to some monosubstituted aromatics (aniline, bromobenzene, and nitrobenzene) and the unimolecular decay of the adducts. Part 2. Kinetics into a quasi-equilibrium, *J. Phys. Chem.*, 90, 3251-3259, <https://doi.org/10.1021/j100405a040>, 1986.
- Xie, M., Chen, X., Hays, M. D., and Holder, A. L.: Composition and light absorption of N-containing aromatic compounds in organic aerosols from laboratory biomass burning, *Atmos. Chem. Phys.*, 19, 2899-2915, <https://doi.org/10.5194/acp-19-2899-2019>, 2019.
- Xu, Y., Dong, X. N., He, C., Wu, D. S., Xiao, H. W., and Xiao, H. Y.: Mist cannon trucks can exacerbate the formation of water-soluble organic aerosol and PM_{2.5} pollution in the road environment, *Atmos. Chem. Phys.*, 23, 6775-6788, <https://doi.org/10.5194/acp-23-6775-2023>, 2023.
- Yang, T., Xu, Y., Ye, Q., Ma, Y. J., Wang, Y. C., Yu, J. Z., Duan, Y. S., Li, C. X., Xiao, H. W., Li, Z. Y., Zhao, Y., and Xiao, H. Y.: Spatial and diurnal variations of aerosol organosulfates in summertime Shanghai, China: potential influence of photochemical processes and anthropogenic sulfate pollution, *Atmos. Chem. Phys.*, 23, 13433-13450, <https://doi.org/10.5194/acp-23-13433-2023>, 2023.

- Yao, L., Wang, M. Y., Wang, X. K., Liu, Y. J., Chen, H. F., Zheng, J., Nie, W., Ding, A. J., Geng, F. H., Wang, D. F., Chen, J. M., Worsnop, D. R., and Wang, L.: Detection of atmospheric gaseous amines and amides by a high-resolution time-of-flight chemical ionization mass spectrometer with protonated ethanol reagent ions, *Atmos. Chem. Phys.*, 16, 14527-14543, 10.5194/acp-16-14527-2016, 2016.
- Zhang, X., Krechmer, J. E., Groessl, M., Xu, W., Graf, S., Cubison, M., Jayne, J. T., Jimenez, J. L., Worsnop, D. R., and Canagaratna, M. R.: A novel framework for molecular characterization of atmospherically relevant organic compounds based on collision cross section and mass-to-charge ratio, *Atmos. Chem. Phys.*, 16, 12945-12959, <https://doi.org/10.5194/acp-16-12945-2016>, 2016.
- Zhao, Y., Yao, M., Wang, Y., Li, Z., Wang, S., Li, C., and Xiao, H.: Acylperoxy Radicals as Key Intermediates in the Formation of Dimeric Compounds in α -Pinene Secondary Organic Aerosol, *Environ. Sci. Technol.*, 56, 14249-14261, <https://doi.org/10.1021/acs.est.2c02090>, 2022.
- Zhong, S., Chen, S., Deng, J., Fan, Y., Zhang, Q., Xie, Q., Qi, Y., Hu, W., Wu, L., Li, X., Pavuluri, C. M., Zhu, J., Wang, X., Liu, D., Pan, X., Sun, Y., Wang, Z., Xu, Y., Tong, H., Su, H., Cheng, Y., Kawamura, K., and Fu, P.: Impact of biogenic secondary organic aerosol (SOA) loading on the molecular composition of wintertime PM_{2.5} in urban Tianjin: an insight from Fourier transform ion cyclotron resonance mass spectrometry, *Atmos. Chem. Phys.*, 23, 2061-2077, <https://doi.org/10.5194/acp-23-2061-2023>, 2023.